OXFORD

Research Article

Mouse oocytes connect with granulosa cells by fusing with cell membranes and form a large complex during follicle development[†]

Kouji Komatsu* and Satoru Masubuchi

Department of Physiology, Aichi Medical University, Nagakute, Aichi, Japan

*Correspondence: Department of Physiology, Aichi Medical University, 1-1 Yazakokarimata, Nagakute, Aichi 480-1195, Japan E-mail: komatsu.kouji.121@mail.aichi-med-u.ac.jp

Abstract

Proper development and maturation of oocytes requires interaction with granulosa cells. Previous reports have indicated that mammalian oocytes connect with cumulus cells through gap junctions at the tip of transzonal projections that extend from the cells. Although the gap junctions between oocytes and transzonal projections provide a pathway through which small molecules (<1 kDa) can travel, it is unclear how molecules >1 kDa are transported between the oocytes and cumulus cells. In this study, we presented new connections between oocytes and granulosa cells. The green fluorescein protein *Aequorea coerulescens* green fluorescein protein (AcGFP1) localizing in oocyte cell membrane, 1,1′-dioctadecyl-3,3,3′,3′-tetramethylindocarbocyanine perchlorate and dextran conjugates (10,000 MW) injected into the oocytes, which were unable to pass through gap junctions, were diffused from the oocytes into the surrounding granulosa cells through these connections. These connect an oocyte to the surrounding cumulus and granulosa cells by fusing with the cell membranes and forming a large complex during follicle development. Furthermore, we show two characteristics of these connections during follicle development—the localization of growth and differentiation factor-9 within the connections and the dynamics of the connections at ovulation. This article presents for the first time that mammalian oocytes directly connect to granulosa cells by fusing with the cell membrane, similar to that in *Drosophila*.

Summary Sentence

An oocyte connects with surrounding granulosa cells by fusing with cell membranes. These connections are important for transportation between the oocyte and granulosa cells and for ovulation.

Key words: oocyte, cumulus cell, granulosa cell, follicle, follicular development, ovulation.

Introduction

The process of oocyte development is supported by granulosa and theca cells [1–7], and the bidirectional communication between an oocyte and granulosa cells is important for the development and maturation of the oocyte. As early as 1976, Anderson et al. reported that oocytes are connected to companion cells through gap junctions in mouse, rat, rabbit, and primate models [8], and several roles for

these connections have subsequently been reported. For example, cyclic guanosine monophosphate, supplied by cumulus cells through the gap junctions, controls oocyte meiotic arrest [5]. In mice lacking connexin 37, which is a gap junction protein, the gap junctions between the oocytes and transzonal projections (TZPs) were ablated, and oogenesis and follicular development were abnormal [9]. Thus, gap junctions represent key communication pathways that control

the development of oocytes and follicles [5, 6, 10]. On the other hand, *Drosophila* oocytes are linked to 15 nurse cells by an intercellular bridge called a ring canal [11, 12]. Transcription in the *Drosophila* oocyte is inactive during oogenesis, and most of the mRNAs and proteins that are required for development are produced and transported from the linked nurse cells through the ring canal [13].

We examined the follicular development in mouse ovaries using time-lapse images of cultured ovarian tissue that was extracted from mice containing the transgenes *oogenesin 1 (Oog1) pro3.9* and ROSA26 (*R26*)-*H2B-mCherry* [14–17]. Through this original culture method, we were able to observe the process from follicle development to ovulation in vitro [17]. *Oog1* is an oocyte-specific gene in the ovaries that is expressed after the start of meiosis [14], and *Oog1pro3.9* mice contain a transgene that connects the *Oog1* promoter to a gene in the *Aequorea coerulescens* green fluorescein protein (AcGFP1). The AcGFP1 signal is detected in the transgenic oocytes beginning in the primordial follicle stage [15]. This gene also contains a neuromodulin fragment that targets AcGFP1 to the plasma membrane; therefore, AcGFP1 should be expressed only in oocyte membranes in transgenic mice. However, we found that AcGFP1-positive projections were elongated from the oocytes to the granulosa-cell area, for example, with neuron dendrites. In this study, we analyzed the structure of the projections, and clarified that oocytes connect with surrounding granulosa cells by fusing with the cell membrane. These connections were sustained in the cumulus–oocyte complexes during follicle development, so we named them connections in the cumulus-oocyte complex (CCOCs). Here we provide the characteristics and roles of CCOCs during follicle development.

Materials and Methods

Animals

All mice used in our experiments were housed in an environmentally controlled room maintained at $23 \pm 1°C$ with a 12 h light/12 h dark cycle. Animal care and the experiments using them were conducted in accordance with the Guidelines for Animal Experimentation, Aichi Medical University, Japan, and were approved by The Animal Care and Use Committee, Aichi Medical University (Experimental No.1150). In this report, two types of transgenic mice were used-*Oog1pro3.9* mice, provided by the RIKEN BioResource Center through the National Bio-Resource Project of the Ministry of Education, culture, Sports and Technology (MEXT), Japan (Accession No. BRC06134), and *R26-H2B-mCherry* mice, provided by the RIKEN Center for Life Science Technologies (Accession No. CDB.0239K, http://www.clst.riken.jp/arg/reporter_mice.html). All transgenic mice were backcrossed to a C57BL/6 strain. Polymerase chain reaction (PCR) genotyping of each transgenic mouse was as previously reported [15, 16].

Ovarian tissue culture

The ovarian tissue of a 4-week-old *Oog1pro3.9/R26-H2B-mCherry* female mouse was sliced into four pieces and cultured on a cell-culture insert. The culture conditions and detailed methods we used were as reported previously [17].

Imaging of cultured ovarian slices

Time-lapse images of cultured ovarian slices were captured at 30 min intervals using a CellVoyager CV1000 confocal scanner box (Yokogawa Electric Corporation).The Z-step size was 5 μm, and the Z-stack thickness was ~150 μm.

Ovary cryosection stains

Tissue sections were obtained by embedding the ovaries of 3- and 6-month-old female mice in optical cutting temperature compound (Sakura Finetek). The ovaries were then frozen in liquid nitrogen and cut to a thickness of 12 μm using a cryostat, CM 3050S (Leica Biosystems), before being fixed in 4% paraformaldehyde (Nacalai Tesque, Inc.) for 20 min on ice and washed with Ca^{2+}- and Mg^{2+}-free phosphate buffered saline (PBS). Cryosections were treated with PBS containing 0.1% Triton X-100 for 10 min, and blocked with Blocking One (Nacalai Tesque, Inc.) at room temperature (RT). Sections were then incubated overnight with a chick anti-green fluorescent protein (GFP) antibody (1:500 dilution; product no. ab13970; Abcam, Inc.), or both of an anti-GFP antibody and a rabbit anti-growth and differentiation factor-9 (GDF-9) antibody (1:200 dilution; product no. ab93892; Abcam, Inc.), at 4°C, after which they were washed four times with PBS. The sections were then incubated at RT for 90 min with goat anti-chick antibody Alexa Fluor 488 (1:500 dilution; product no.150169; Abcam, Inc.), rhodamine phalloidin (1:1000 dilution; Thermo Fisher Scientific), and DAPI (1:1000 dilution, SIGMA-Aldrich Corporation) (Figures 1 and 3), or with goat anti-chick antibody Alexa Fluor 488, goat anti- rabbit antibody Alexa Fluor 594 (1:500 dilution; product no. ab150080; Abcam, Inc.), and DAPI (Figure 6). Following incubation, the sections were washed four times with PBS and cover-slipped with Vectashield mounting medium (VECTOR Laboratories), before images were captured using the LSM710 confocal microscope (Carl Zeiss Microimaging Co., Ltd).

Injection of DiI and dextran conjugated with Alexa594 into oocytes

Dextran conjugated with Alexa Fluor 594 (Abcam, Inc.) was injected into the oocytes of the cultured ovaries using a microinjector (Eppendorf). The tissues were cultured for 46 h, after which their images were captured using confocal microscopy. Water-resistant gel paste containing CM-1,1'-dioctadecyl-3,3,3',3'-tetramethylindocarbocyanine perchlorate (DiI, Thermo Fisher) was embedded into oocytes in 14-μm-thick cryosections, and their time-lapse images were captured at 10-min intervals using confocal microscopy, with a Z-step size of 2 μm.

Electron microscopy

The ovaries of postnatal-day-4 wild-type (WT) female mice were fixed overnight using 2% paraformaldehyde and 2% glutaraldehyde (Electron Microscopy Sciences) in 0.1 M phosphate buffer (PB, pH 7.4) at 4°C. Following fixation, the samples were washed three times with 0.1 M PB for 30 min, and fixed with 2% osmium tetroxide in 0.1 M PB for 2 h at 4°C. Samples were dehydrated in graded ethanol solutions (50%: 20 min at 4°C; 70%: 20 min at 4°C; 90%: 20 min at RT; 100%: 20 min at RT), infiltrated twice with propylene oxide (PO) for 30 min, and added to mixed solutions of 70% PO and 30% resin (Nisshin EM Co.) for 1 h. Sample tube caps were left open overnight to evaporate the volatile PO, before the samples were transferred into 100% resin and polymerized for 48 h at 60°C. Polymerized resin samples were cut into 70-nm sections using a diamond knife and ultramicrotome (Leica Biosystems). The sections were then stained with 2% uranyl acetate for 15 min at RT, washed with distilled water, and then stained with lead stain solution (Sigma-Aldrich Corporation) for 3 min at RT. The stained sections were analyzed using a transmission electron microscope (JEOL Ltd), and their images were captured using a charge-coupled device camera (JEOL Ltd).
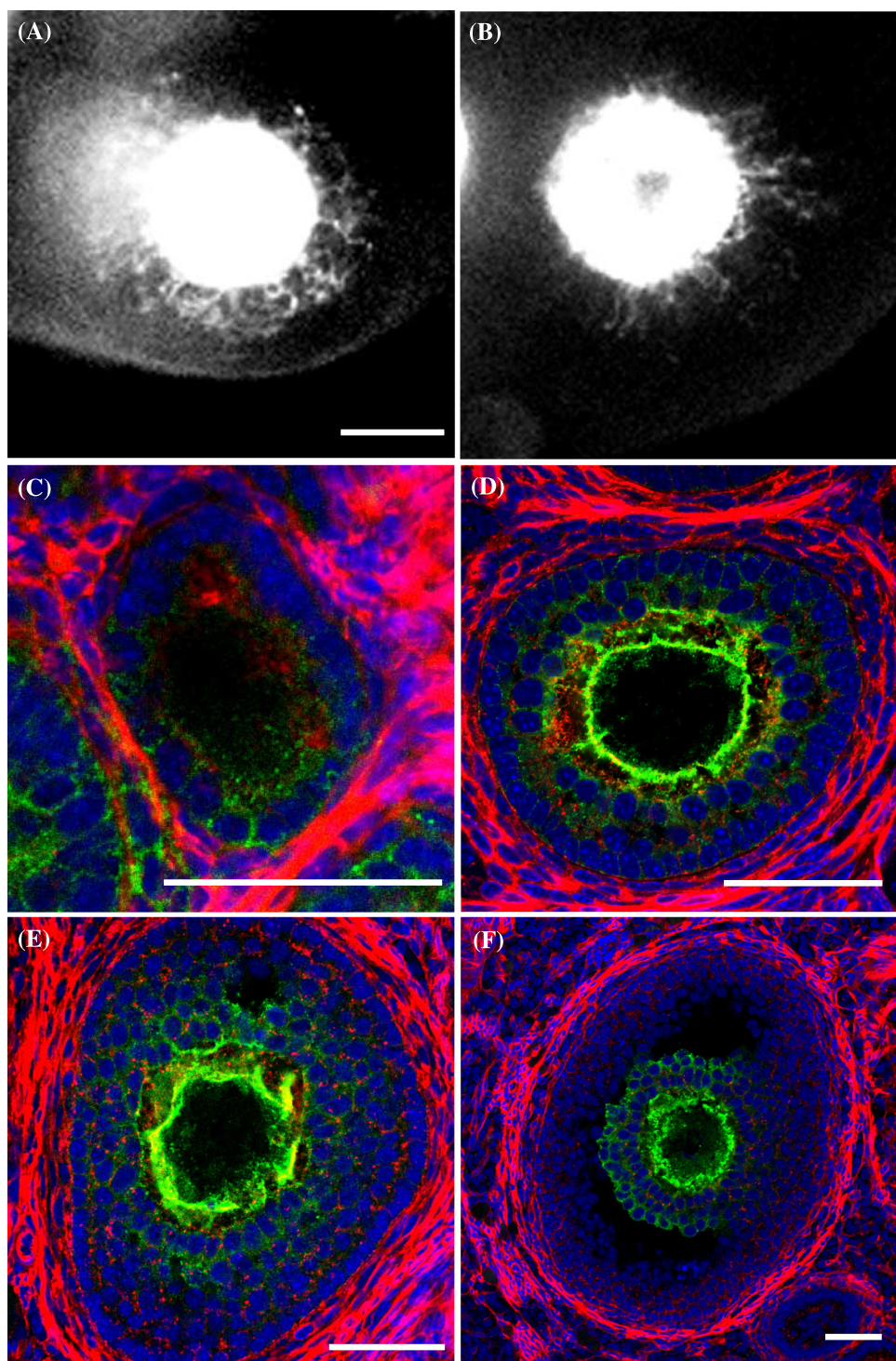
Figure 1. Localization of AcGFP1 in the follicle and the cumulus-oocyte complex. (A and B) Follicles expressing AcGFP1 in the cultured ovary of an *Oog1pro3.9* mouse. (C–F) Follicles stained using anti-GFP antibody (green), phalloidin (red), and DAPI (blue). (C) Primary follicle. (D) Secondary follicle. (E) An early antral follicle. (F) Graafian follicle. Scale bars, 50 μm.

Immunoelectron microscopy

The ovaries of 10-week-old *Oog1pro3.9* mice were fixed with 4% paraformaldehyde and 0.1% glutaraldehyde (Electron Microscopy Sciences) in 0.1 M PB (pH 7.4) for 1 h at 4°C, after which they were washed three times for 15 min each in 0.1 M PB. The fixed ovaries were then dehydrated in 50% and 70% ethanol solutions for 30 min at 4°C before being infiltrated three times with a mixture of ethanol and resin (1:1) for 30 min at 4°C. Samples were then transferred to fresh 100% resin and subjected to ultraviolet polymerization overnight at 4°C. The ovaries embedded in

polymerized resin were sliced into ultrathin 80-nm sections using a diamond knife and ultramicrotome (Leica Biosystems) and mounted on nickel grids. Sections were then incubated overnight at 4°C with rabbit anti-GFP antibody (Abcam, Inc.) in PBS containing 1% bovine serum albumin (BSA), washed three times for 1 min each with 1% BSA/PBS, and incubated with anti-rabbit IgG antibody conjugated with 10 nm gold particles for 2 h at RT. Following the three PBS washes, the sections were fixed in 2% glutaraldehyde in 0.1 M PB, dried, and then were stained for 15 min with 2% uranyl acetate. Lastly, the sections were stained with lead stain solution (SIGMA-Aldrich Corporation) for 3 min at RT, and images of the stained sections were captured using the JEM-1400plus transmission electron microscope (JEOL Ltd).

RNA isolation, cDNA synthesis, and reverse transcription PCR

The oocytes and surrounding granulosa cells were removed from the cryosections of the *Oog1pro3.9* and WT female mouse ovary using PALM Micro Tweezers (Carl ZEISS Microimaging Co., Ltd). Total RNA was then extracted from 20 dissected tissues using the RNeasy Micro Kit (QIAGEN Company), Following the manufacture's protocol, the cDNA from each sample was synthesized using the SuperScript III First-Strand Synthesis system (Invitrogen Corporation). Finally, to confirm *Oog1* and *AcGFP1* mRNA expression in the oocytes and granulosa cells from each mouse line, synthesized cDNA was subjected to PCR on PCR Thermal Cycler Dicer (Takara Bio), following the protocols outlined in previous reports [14, 15].

Western blotting

Four ovaries obtained from two 30-day-old C57BL/6 female mice were homogenized in 100 μL lysis buffer (Tissue Extraction Reagent I, Invitrogen Corporation) containing EDTA-free protease inhibitor cocktail (Clontech). The extract was then centrifuged at 15,000 rpm for 10 min at 4°C. Each 5 μL sample, the supernatant and mouse recombinant GDF-9 (product no. 739-G9/CF, R&D Systems, Inc.) diluted in lysis buffer, was mixed with 5 μL sample buffer containing 2-mercaptoethanol (Bio-Rad), and was boiled for 5 min at 95°C. Each sample was separated using 10% SDS acrylamide gel electrophoresis, and transferred to a polyvinylidene difluoride membrane (Bio-Rad). The membrane was blocked in Blocking One (Nacalai Tesque, Inc.) for 20 min, then incubated with anti-GDF-9 antibody (1:1000 dilution; product no. ab93892; Abcam, Inc.) at RT for 1 h. After washing in tris-buffered saline and polysorbate (Tween 20; TBST), the membrane was incubated with goat anti-rabbit antibody HRP conjugate (Bio-Rad) at RT for 1 h, and then washed again in TBST. Chemiluminescence was detected using Clarity Western ECL substrate (Bio-Rad), and the image was captured using Amersham Imager 600 (GE Healthcare).

Results

AcGFP1 is transferred from oocytes to granulosa cells

On examining the time-lapse images of cultured *Oog1pro3.9* mouse ovaries, elongated projections were observed on the oocytes (Figures 1A and B, and Supplemental Movie S1). The AcGFP1 signal was saturated on Figure1A and B because the images were captured to observe the projections under specific time-lapse condition. The signal in the granulosa cells was lower than that in the oocytes;

therefore, the projection was not detected under normal capturing condition (Supplemental Figure S1).

To observe the detailed structure of the AcGFP1-positive projections (Figure 1A and B), we stained cryosections of *Oog1pro3.9* mouse ovaries with anti-GFP antibody (Figure 1C–F) for immunohistochemical analyses. These results clearly showed that AcGFP1 was localized in the cell membrane of granulosa cells, as with the oocytes. AcGFP1 was localized in all granulosa cells at the primary and secondary follicle stages (Figure 1C and D), while it was localized only in cumulus cells after the antral follicle stage (Figure 1E and F), and disappeared from these cells after ovulation (data not shown). Not all primary follicles were AcGFP1 positive (4/8); however, AcGFP1 was found in the granulosa or cumulus cells in all of secondary and antral follicles (secondary follicle: 30/30, antral follicle: 29/29). AcGFP1 expression level increased as the follicles grew; therefore, we could not detect the AcGFP1 signal in the early primary follicle stage.

We confirmed that *Oog1* and *AcGFP1* mRNAs were expressed in the oocytes (Supplemental Figure S2); however, AcGFP1 protein localized to both the oocytes and granulosa cells. These results indicate that AcGFP1 was transferred to the granulosa cells from the oocytes.

DiI and dextran-Alexa Fluor 594 conjugates transferred from oocytes to granulosa cells via an interconnection

We injected DiI into the oocytes of the ovarian cryosections of a WT mouse to determine how AcGFP1 in the oocyte membrane was transferred to granulosa cells (Figure 2A). DiI could not pass through gap junctions and instead spread along the cell membranes[18], similar to how AcGFP1 spreads within the follicles of *Oog1pro3.9* mice. DiI injected into the oocytes diffused through the connections between the oocytes and the granulosa cells (Figure 2B–H). To confirm whether DiI spread from an oocyte on which cell membrane was broken by freezing or sectioning, we injected DiI on the oocytes of ovarian cryosections from *Oog1pro3.9* mice (Supplemental Figure S3). The DiI signal merged with the AcGFP1 signal but did not spread beyond the AcGFP1-positive area in the follicle (7/7). This result provided the evidence that DiI spread through CCOCs in the same way as AcGFP1 in the follicle and not by leaking from the damaged oocyte membrane (Supplemental Figure S3), which also indicated that there are connections by which DiI can be transferred between oocytes and granulosa cells (Figure 2D–H). In fact, there were two types of connections, phalloidin-positive TZPs and phalloidin- and AcGFP1-positive CCOCs (Figure 3A–D). Furthermore, data from immunoelectron microscopy images showed AcGFP1-positive and AcGFP1-negative connections (Figure 3E–H). At the gap junctions, little AcGFP1 was detected in TZPs. On the other hand, a large amount of AcGFP1 was localized in the elongated projection extending from the oocyte (Figure 3F and G). These results show new connections between an oocyte and granulosa cells through which AcGFP1 can pass.

Next, to further determine whether substances in the cytoplasm can diffuse from the oocytes into granulosa cells, we injected dextran conjugated with Alexa Fluor 594 (10 000 MW), which cannot pass through gap junctions, into five oocytes of secondary or antral follicles in cultured ovarian tissue (Figure 4). Although two of the five follicles continued to grow, damage from the injection prevented the growth of the others (data not shown). After injecting the dextran conjugated with Alexa 594 and culturing for 46 h, its diffusion was confirmed in both growing follicles (Figure 4C and D), indicating
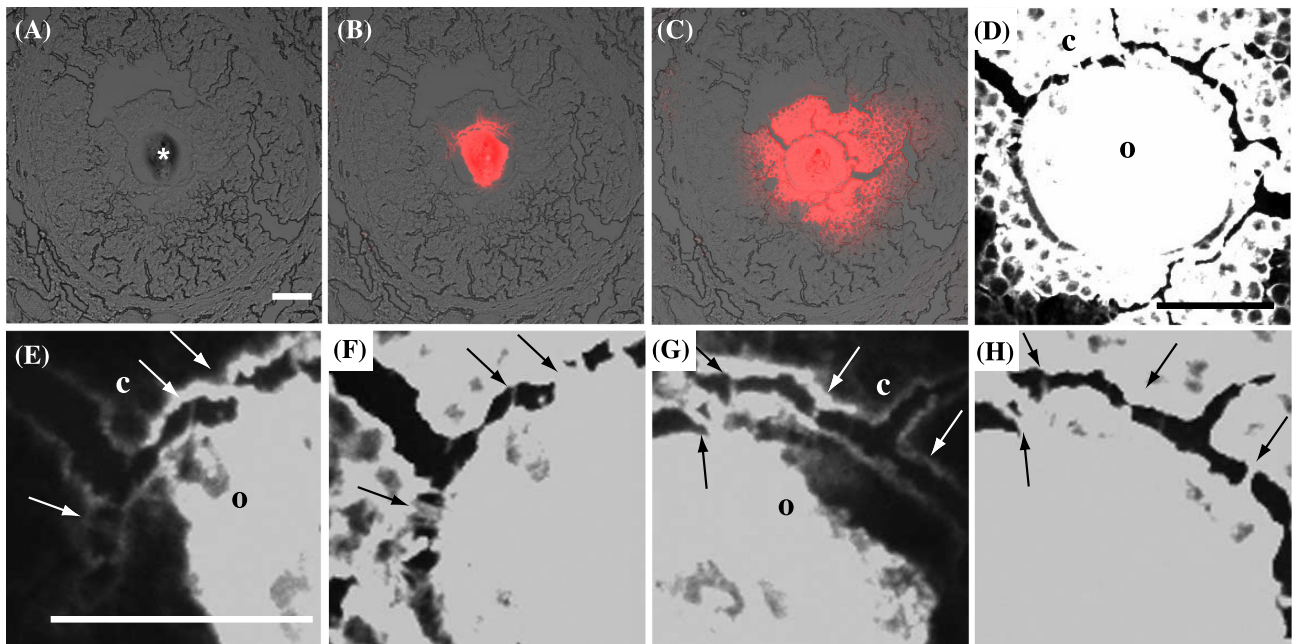
Figure 2. Water-resistant gel paste containing DiI injected onto the oocyte in the prepared cytosection of the ovary. (A, B, E, G) 1 h after injection. (C, D, F, H) 10 h after injection. (E–H) Enlarged images between the oocyte and granulosa cells in (D), (E) and (F), (G) and (H) are at the same location. The asterisk in (A) denotes injected water-resistant gel paste containing DiI. The arrows in (E–H) indicate CCOCs between the oocytes and granulosa cells. DiI is red in (B) and (C), and white in (D–H). Notes: o, oocyte. c, cumulus cell. Scale bar, 50 μm.

that the substances localized in the cytoplasm are also able to pass through CCOCs, as is seen with both AcGFP1 and DiI.

Oocytes connect with granulosa cells and granulosa cells connect with each other by fusing with the cell membrane

To elucidate the structure of CCOCs, we examined ovarian follicles using an electron microscope. In this experiment, we focused on the primary follicles because TZPs and CCOCs were winding into the zona pellucida after the secondary follicle stage, making it difficult to clearly identify their entire structure (Figure 3E). The data showed the existence of a direct connection between the oocytes and granulosa cells by fusing with the cell membrane (Figure 5A and B). Moreover, the results showed that granulosa cells also connect with each other through this fusion (Figure 5C and D), which indicates that oocytes and surrounding granulosa cells share cytoplasm with CCOCs and form a large cellular complex during follicle development.

Two types of projections developed in the primary follicle stage—one from granulosa cells to an oocyte and the other from an oocyte to a granulosa cell (Figure 5E–G). Fusion with cell membrane was formed mainly at the projections from the oocytes to the granulosa cells in the primary follicles (4/11, Figure 5B), and not at the projections from the granulosa cells to the oocytes (0/14, Figure 5F).

The role of CCOCs during follicle development and ovulation

We confirmed GDF-9 was localized in the follicles of *Oog1pro3.9* mice (Figure 6A–C). This important protein is secreted by the oocytes and controls the proliferation of granulosa cells during follicle development [19]. Immunohistochemistry showed that GDF-9 is localized in the oocytes, granulosa cells, and CCOCs (Figure 6B and

C). The specificity of anti-GFP and GDF-9 antibody was confirmed (Supplemental Figure S4). The anti-GDF-9 antibody detected mainly pro-mature GDF-9 in the mouse ovary extract (Supplemental Figure S4B); therefore, it is speculated that most of the signals in Figure 6A–C represent the localization of pro-mature GDF-9 in the oocytes and granulosa cells [20]. This result suggests that large molecules can be transported through CCOCs to control oocyte and follicle development.

Our time-lapse movie of an ovary from *Oog1pro3.9/H2B-mCherry* mouse showed that a strong AcGFP1 signal elongates from the oocytes in a specific direction at ovulation, coincident with the ovulation route (Figure 6D–K and Supplemental Movie S2). In the three cultured ovarian tissues, 12 oocytes had ovulated, and the elongated projection was seen on 10 of 12; however, the projections can be seen only if the intensity of AcGFP1 is sufficient. Thus, the expression level intensity of AcGFP1 in the two oocytes in which AcGFP1-positive projections were not observed might has been low. Because the cumulus cells connect with oocytes through CCOCs (Figure 1F), these elongated projections revealed that cumulus cells move in the direction of ovulation and pull the oocyte in that same direction.

Discussion

In this study, the identification of CCOCs depended on AcGFP1 and DiI localization within the plasma membrane. AcGFP1 and DiI were localized in oocyte cell membranes and could not be transferred through the gap junctions. From these results, we considered the following three possibilities: (1) *AcGFP1* mRNA is transferred from oocytes to granulosa cells; (2) oocyte cell membranes are directly connected with those of granulosa cells by fusing with cell membrane, or (3) oocyte membranes are transported to granulosa cells by exosomes [6]; however, *AcGFP1* mRNA expressed only in
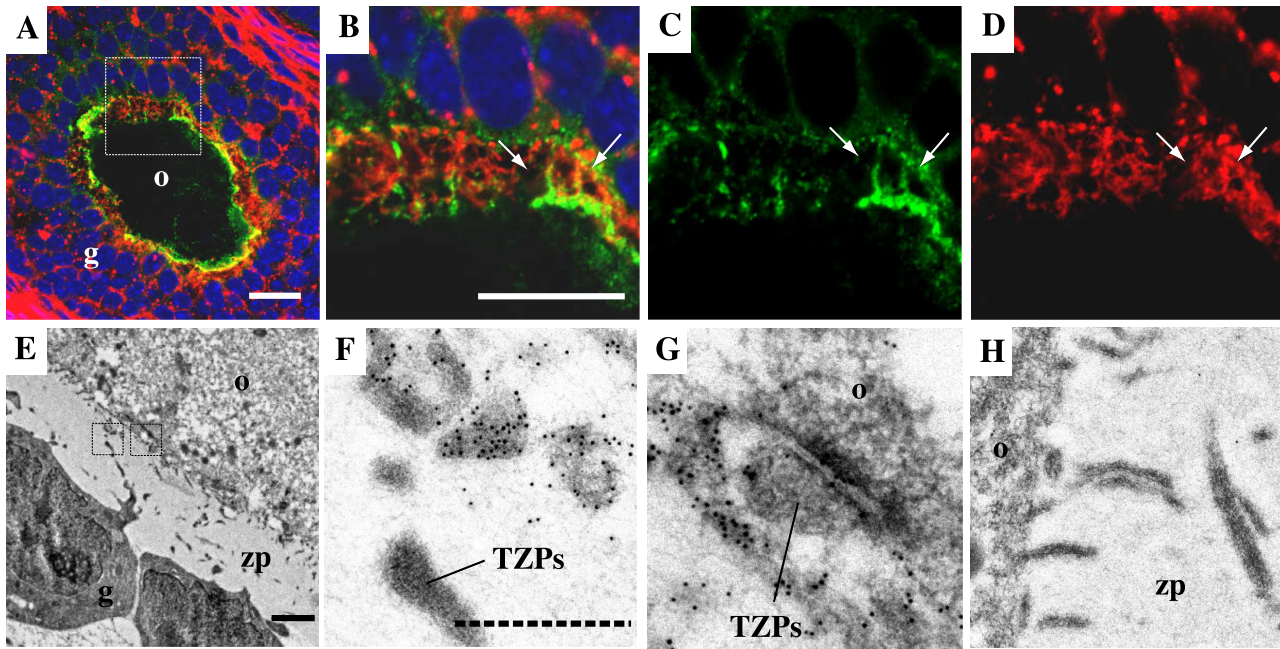
Figure 3. Localization of AcGFP1 in CCOCs and TZPs. (A–D) Immunohistochemistry images. Anti-GFP antibody (green), phalloidin (red), and DAPI (blue). (B, C, D) Elongated images of the square area in (A). Arrows indicate AcGFP1-positive CCOCs. (E–H) Immunoelectron microscope images between an oocyte and granulosa cells. Black dots denote the signal of anti-GFP antibody. (F, G) Enlarged images of the area enclosed by a square in (E), respectively. (H) Negative control stained rabbit IgG. Notes: o, oocyte. g, granulosa cell. zp, zona pellucida. TZPs, transzonal projections. The white scale bar in (A) and (B): 20 μm; the black line in (E): 1 μm; the dashed line in (F): 200 nm.
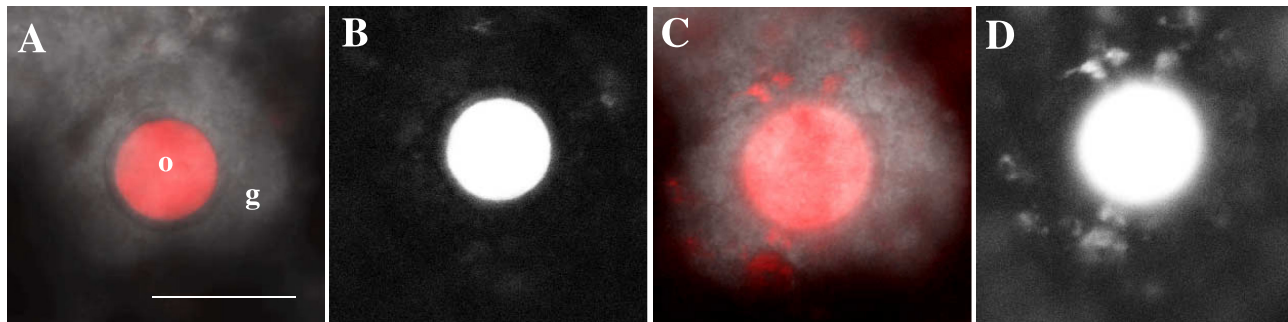

Figure 4. Dextran conjugates with Alexa594 injection in the oocyte of a cultured ovary. (A, B) 1 h after injection. (C, D) 46 h after injection. Dextran conjugates are red in (A) and (C) and are white in (B) and (D). Notes: o, oocyte. g, granulosa cell. Scale bar, 50 μm.

the oocytes (Supplemental Figure S2), and the oocytes in the cryosections, could not release exosomes (Figure 2), so we concluded that oocytes and granulosa cells are connected through cell-membrane fusion. Using *Oog1pro3.9* mouse ovary, we then found that there are connections other than gap junctions through TZPs, and that AcGFP1 diffuses through them (Figures1 and 3, and Supplemental Movie S1). It is difficult to distinguish between CCOCs and TZPs using conventional experimental methods, including electron microscopy and immunohistochemistry, because their structures are nearly the same (Figure 3).

In primary follicles, AcGFP1 had already diffused from the oocytes to the granulosa cells (Figure 1C), so CCOCs had already formed in those follicles (Figures 1 and 5); however, it was not clear in this study whether primordial follicles contained CCOCs because the expression of AcGFP1 was low in these follicles, and CCOCs were not found using electron microscopy. If CCOCs are formed from the primary follicle stage, their formation might correlate with

the quiescence and activation of primordial follicles. It remains unclear how the quiescent primordial follicles in the ovary are activated, but formation of CCOCs might provide a clue.

In the primary follicle stage, CCOCs and TZPs are very short because the zona pellucida is not yet formed (Figure 5). Two types of projections were formed in these follicles (Figure 5E–G). CCOCs were formed at the projection that connected the oocytes to the granulosa cells; therefore, we speculated that these projections formed CCOCs (Figure 5G), while the projections from the granulosa cells to the oocytes formed TZPs (Figure 5F). The detailed structure of CCOCs is not clear, but the electron microscope image showed that the cell membrane was directly fused between an oocyte and the granulosa cells and no specific structure was observed (Figure 5B).

The diffusion of enhanced cyan fluorescent protein (ECFP) from the oocytes to the granulosa cells was observed in follicles that were reconstructed in vitro (Hayashi K, personal communication)
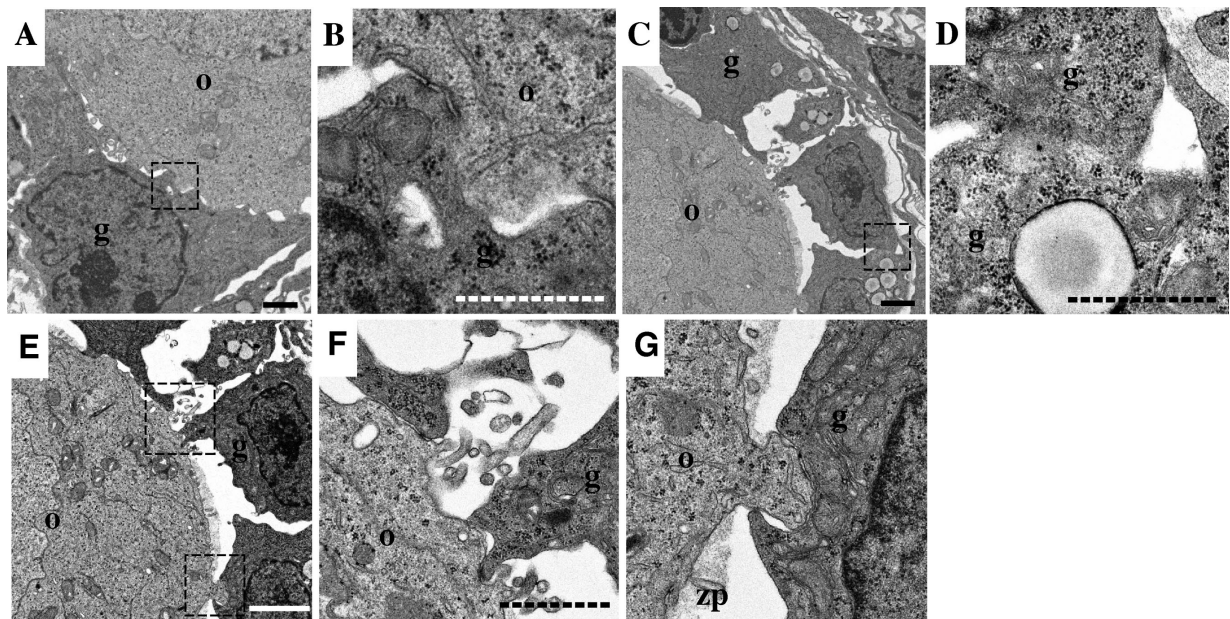
Figure 5. Electron microscope images. (A–G) Between an oocyte and the granulosa cells in the primary follicles. (B, D, F, G) Enlarged images of the area enclosed by a square in (A), (C), and (E), respectively. Notes: o, oocyte. g, granulosa cell. zp, zona pellucida. Scale bars, 2 μm (line) and 1 μm (dashed line).

[21]. The oocytes in the follicles were derived from the embryonic stem cell line, BVSCH18, that contains the transgenes *Blimp-mVenus* and *stella-ECFP,* and the granulosa cells were derived from gonadal somatic cells of the albino ICR (named after the Institute of Cancer Research) strain mice; therefore, the ECFP in the granulosa cells must have been transferred from the oocytes. These results support the results in our study and show that CCOCs are formed by contact between oocytes and pre-granulosa or granulosa cells, and that substances in the oocytes can be transferred into the granulosa cells in much the same way as dextran conjugates injected into the oocyte (Figure 4). Our study showed that the substances in the cell membrane (AcGFP1 and DiI) and in the cytoplasm of the oocytes (dextran conjugates and GDF-9) can be transferred into the granulosa cells. AcGFP1, DiI, and dextran conjugates might freely diffuse through CCOCs, but a regulatory mechanism of transportation is needed for GDF-9 and other factors to be able to correctly control the growth of oocytes and granulosa cells. In fact, *AcGFP1* mRNA does not diffuse from the oocytes into the granulosa cells (Supplemental Figure S2). To understand the mechanism of oocyte development and maturation, the roles and regulatory mechanisms of transport through CCOCs must be elucidated.

The number of CCOCs is lower than the number of TZPs (Figure 3B); however, CCOCs connect the oocyte and all the granulosa cells in the follicle at the primary and secondary follicle stages, and all cumulus cells at the antral and Graafian follicle stages (Figure 1C–F). It is considered that granulosa cells differentiate into cumulus and mural granulosa cells at the antral follicle stage, and that paracrine factors secreted from oocytes inhibit the differentiation of cumulus cells into mural granulosa cells [22]. Our results show that proteins in the cytoplasm can pass through CCOCs; therefore, the differentiation of granulosa cells might be controlled through CCOCs, by limiting the distribution of key differentiation factors for cumulus cells.

Although the mechanism by which oocytes physically ovulate from a follicle has not yet been revealed, our results highlight the sequence of events that take place in the follicle during this time (Figure 6D–K and Supplemental Movie S2). First, the basement membrane of the follicle is first degraded by proteolysis [23–25]. Then, the cumulus cells move out from the cleavage point and the oocyte is pulled by the cumulus cells out of the follicle (Supplemental Movie S2). It is not clear how the movement of cumulus cell is induced to move, but our results confirm that oocyte movement is physically controlled by these cells and CCOCs at ovulation.

Previous reports have presented the importance of communication between an oocyte and the surrounding cumulus cells through TZPs. An oocyte stimulates the metabolism and growth of granulosa cells through paracrine factors, bone morphogenetic protein 15, and GDF-9. On the other hand, transportation of small molecules, cAMP, and amino acid from granulosa cells into an oocyte through TZPs controls oocyte meiosis and oocyte maturation [26–28]; however, the zona pellucida separates an oocyte and the granulosa cells, so it is not clear how large molecules are correctly transported. In this article, we present that CCOCs connect the oocytes to the surrounding granulosa cells, forming a huge complex that then nurtures the oocytes. This structure has many other advantages, such as storing large amounts of maternal factors within an oocyte, and controlling the development and maturation of the oocytes in response to physiological changes in the ovary. Thus, in addition to the role of CCOCs identified in our results, they must also perform various important roles in the regulation of oocyte development and maturation. Our results lay the foundation for future research on the development and maturation of the mammalian oocyte.

Supplementary data

Supplementary data are available at *BIOLRE* online.

Supplemental Information contains Supplemental Experimental Procedures, two figures and one table are available online.
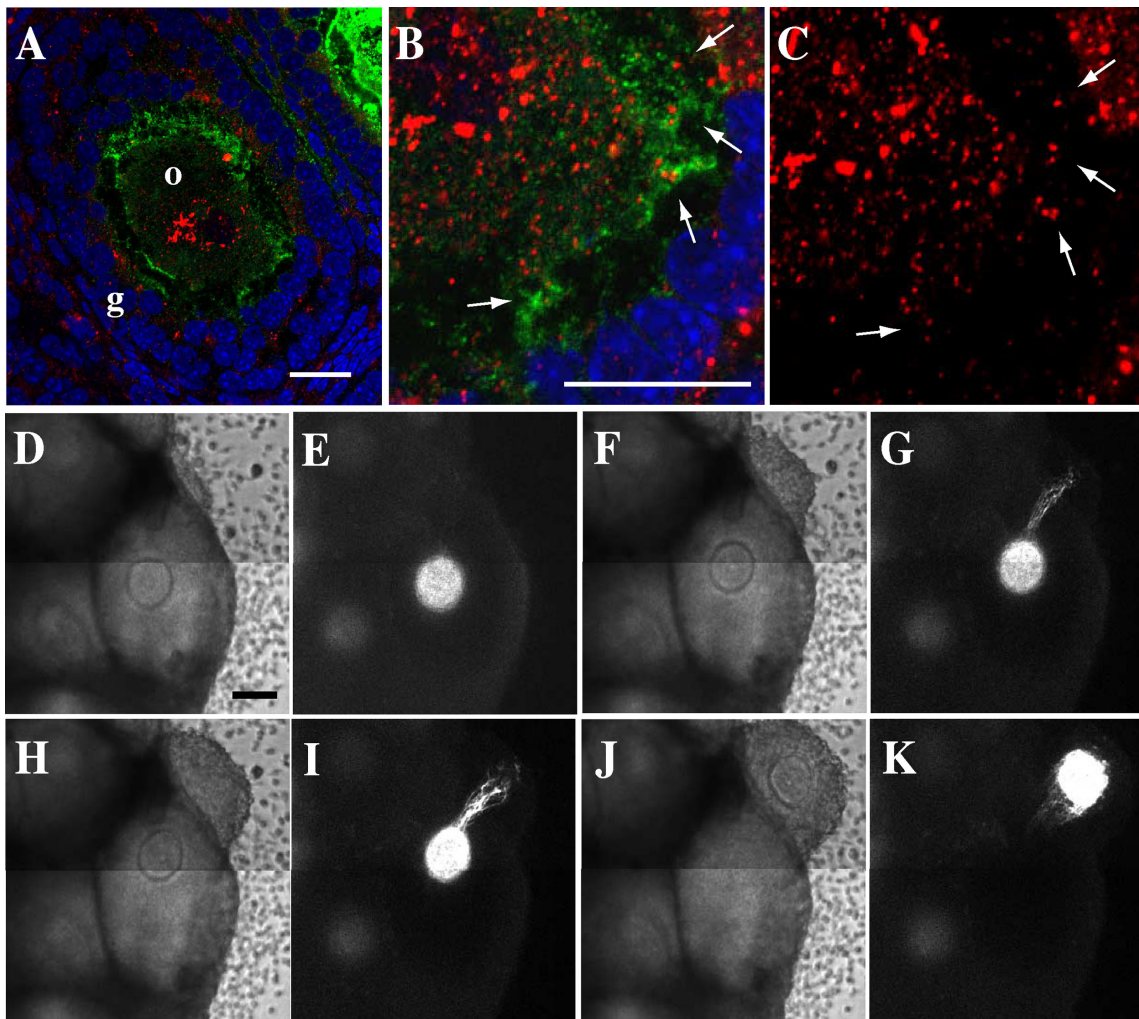
Figure 6. The role of CCOC in follicle development. (A–C) Secondary follicle images stained with anti-GFP antibody (green), anti-GDF-9 antibody (red), and DAPI (blue). The arrows in (B) and (C) denote localization of GDF-9 in AcGFP1-positive CCOCs. (D–K) Time-lapse images of a cultured ovary in a *Oog1pro3.9* mouse. (D, F, H, J) Bright-field images. (E, G, I, K) AcGFP1 images. (D, E) 43 h culture. (F, G) 51 h culture. (H, I) 55 h culture. (J, K) 59 h culture. Notes: o, oocyte. g, granulosa cell. Scale bar, 100 μm.

Supplemental Figure S1. Cultured ovarian tissue of *Oog1pro3.9/R26-H2B-mCherry* mouse. (A–C) Cultured ovarian tissues were obtained from 30-day-old mouse and cultured for 14 days. (A) AcGFP1, (B), mCherry, (C), merged image. Scale bar, 100 μm.

Supplemental Figure S2. *Oog1* and *AcGFP* mRNA expression patterns. Expression of *Oog1* and *AcGFP* mRNA in follicles was checked using PCR, and the samples were microdissected. The purple encircled area in (B) was dissected as an oocyte sample; the purple area in (D) was dissected as a sample of granulosa cells. (A) Intact follicle image. (C) Image after partial oocyte dissection. (E) Image after dissection of a part of granulosa cell area. (F) Electrophoresis image. Notes: Tg denotes samples obtained from *Oog1pro3.9* mouse ovaries. W, samples obtained from mouse ovaries. O, oocyte sample in B. G, sample of granulosa cell in D. Scale bar, 100 μm.

Supplemental Figure S3. Water-resistant gel paste containing DiI injected onto the oocyte in the cryosection of the *Oog1pro3.9* mouse ovary. (A–C) Images of an antral follicle 15 h after injection of water-resistant paste containing DiI. (A) DiI; (B) AcGFP1; (C) merged image of A, B, and bright field. Notes: o, oocyte. Scale bar, 100 μm.

Supplemental Figure S4. Specificity of anti-GFP and anti-GDF-9 antibodies. (A) Secondary follicle in a cryosection of wild type mouse that was stained with anti-GFP antibody (green), phalloidin (red), and DAPI (blue). Notes: o, oocyte. g, granulosa cell. Scale bar, 50 μm. (B) Western blotting for GDF-9 in ovarian extract. A band at 20 kDa is processed mature GDF-9, and a band at $\sim$60 kDa is promature GDF-9 (arrow head). a, mouse recombinant GDF-9 (1 ng, predicted band size: 20 kDa). b, mouse ovarian extract.

Supplemental Movie S1. Time-lapse movie of follicle development in the cultured ovary of *Oog1pro3.9/H2B-mCherry* mouse. The reproducing speed is 10 frames/s. Green. AcGFP1. Red, mCherry.

Supplementary Movie S2. Time-lapse movie of follicle development in the cultured ovary of *Oog1pro3.9/H2B-mCherry* mouse The reproducing speed is 5 frames/s. Green, AcGFP1. Red, mCherry.

References

1. Driancourt MA, Reynaud K, Cortvrindt R, Smitz J. Roles of KIT and KIT LIGAND in ovarian function. *Rev Reprod* 2000; **5**:143–152.

2. Ge L, Han D, Lan GC, Zhou P, Liu Y, Zhang X, Sui HS, Tan JH. Factors affecting the in vitro action of cumulus cells on the maturing mouse oocytes. *Mol Reprod Dev* 2008; **75**:136–142.

3. Norris RP, Ratzan WJ, Freudzon M, Mehlmann LM, Krall J, Movsesian MA, Wang H, Ke H, Nikolaev VO, Jaffe LA. Cyclic GMP from the surrounding somatic cells regulates cyclic AMP and meiosis in the mouse oocyte. *Development* 2009; **136**:1869–1878.

4. Barrett SL, Albertini DF. Cumulus cell contact during oocyte maturation in mice regulates meiotic spindle positioning and enhances developmental competence. *J Assist Reprod Genet* 2010; **27**:29–39.

5. Wigglesworth K, Lee KB, O'Brien MJ, Peng J, Matzuk MM, Eppig JJ. Bidirectional communication between oocytes and ovarian follicular somatic cells is required for meiotic arrest of mammalian oocytes. *Proc Natl Acad Sci USA* 2013; **110**:E3723–E3729.

6. Russell DL, Gilchrist RB, Brown HM, Thompson JG. Bidirectional communication between cumulus cells and the oocyte: old hands and new players? *Theriogenology* 2016; **86**:62–68.

7. Knight PG, Glister C. Local roles of TGF-? superfamily members in the control of ovarian follicle development. *Anim Reprod Sci* 2003; **78**:165–183.

8. Anderson E, Albertini DF. Gap junctions between the oocyte and companion follicle cells in the mammalian ovary. *J Cell Biol* 1976; **71**:680–686.

9. Simon AM, Goodenough DA, Li E, Paul DL. Female infertility in mice lacking connexin 37. *Nature* 1997; **385**:525–529.

10. Gilchrist RB, Ritter LJ, Armstrong DT. Oocyte–somatic cell interactions during follicle development in mammals. *Anim Reprod Sci* 2004; **82–83**:431–446.

11. Mahajan-Miklos S, Cooley L. Intercellular cytoplasm transport during Drosophila oogenesis. *Dev Biol* 1994; **165**:336–351.

12. Cooley L. Drosophila ring canal growth requires Src and Tec kinases. *Cell* 1998; **93**:913–915.

13. Theurkauf WE, Hazelrigg TI. In vivo analyses of cytoplasmic transport and cytoskeletal organization during Drosophila oogenesis: characterization of a multi-step anterior localization pathway. *Development* 1998; **125**:3655–3666.

14. Minami N, Aizawa A, Ihara R, Miyamoto M, Ohashi A, Imai H. Oogenesin is a novel mouse protein expressed in oocytes and early cleavage-stage embryos. *Biol Reprod* 2003; **69**:1736–1742.

15. Ishida M, Okazaki E, Tsukamoto S, Kimura K, Aizawa A, Kito S, Imai H, Minami N. The promoter of the oocyte-specific gene, Oog1, functions in both male and female meiotic germ cells in transgenic mice. *PLoS One* 2013; **8**:e68686.

16. Abe T, Kiyonari H, Shioi G, Inoue K, Nakao K, Aizawa S, Fujimori T. Establishment of conditional reporter mouse lines at ROSA26 locus for live cell imaging. *Genesis* 2011; **49**:579–590.

17. Komatsu K, Koya T, Wang J, Yamashita M, Kikkawa F, Iwase A. Analysis of the effect of leukemia inhibitory factor on follicular growth in cultured murine ovarian tissue. *Biol Reprod* 2015; **93**:18.

18. Honig MG, Hume RI. Fluorescent carbocyanine dyes allow living neurons of identified origin to be studied in long-term cultures. *J Cell Biol* 1986; **103**:171–187.

19. Knight PG, Glister C. TGF- superfamily members and ovarian follicle development. *Reproduction* 2006; **132**:191–206.

20. Watson LN, Mottershead DG, Dunning KR, Robker RL, Gilchrist RB, Russell DL. Heparan sulfate proteoglycans regulate responses to oocyte paracrine signals in ovarian follicle morphogenesis. *Endocrinology* 2012; **153**:4544–4555.

21. Hikabe O, Hamazaki N, Nagamatsu G, Obata Y, Hirao Y, Hamada N, Shimamoto S, Imamura T, Nakashima K, Saitou M, Hayashi K. Reconstitution in vitro of the entire cycle of the mouse female germ line. *Nature* 2016; **539**:299–303.

22. Li R, Norman RJ, Armstrong DT, Gilchrist RB. Oocyte-secreted factor(s) determine functional differences between bovine mural granulosa cells and cumulus cells. *Biol Reprod* 2000; **63**:839–845.

23. Palotie A, Peltonen L, Foidart JM, Rajaniemi H. Immunohistochemical localization of basement membrane components and interstitial collagen types in preovulatory rat ovarian follicles. *Coll Relat Res* 1984; **4**:279–287.

24. Tsafriri A. Ovulation as a tissue remodelling process. Proteolysis and cumulus expansion. *Adv Exp Med Biol* 1995; **377**:121–140.

25. Russell DL, Robker RL. Molecular mechanisms of ovulation: coordination through the cumulus complex. *Hum Reprod Update* 2007; **13**:289–312.

26. Su YQ, Sugiura K, Eppig JJ. Mouse oocyte control of granulosa cell development and function: paracrine regulation of cumulus cell metabolism. *Semin Reprod Med* 2009; **27**:32–42.

27. Eppig JJ, Pendola FL, Wigglesworth K, Pendola JK. Mouse oocytes regulate metabolic cooperativity between granulosa cells and oocytes: amino acid transport. *Biol Reprod* 2005; **73**:351–357.

28. Gilchrist RB, Luciano AM, Richani D, Zeng HT, Wang X, Vos MD, Sugimura S, Smitz J, Richard FJ, Thompson JG. Oocyte maturation and quality: role of cyclic nucleotides. *Reproduction* 2016; **152**: R143–R157.